



An Update to the Boston EEG Automated Processing Pipeline Kalman Detrend Step and an Examination of Mu Suppression

Permanent link

<http://nrs.harvard.edu/urn-3:HUL.InstRepos:38811500>

Terms of Use

This article was downloaded from Harvard University's DASH repository, and is made available under the terms and conditions applicable to Other Posted Material, as set forth at <http://nrs.harvard.edu/urn-3:HUL.InstRepos:dash.current.terms-of-use#LAA>

Share Your Story

The Harvard community has made this article openly available.
Please share how this access benefits you. [Submit a story](#).

[Accessibility](#)

0.2 List of Contributions

The Boston EEG Automated Processing Pipeline (BEAPP) was developed by Dr. A. Levin, A. Mendez Leal and Dr. H. O’Leary. Professor D. Ba developed the Kalman detrend step currently used in BEAPP. The Autism Center of Excellence (ACE Network) involves researchers from Yale, University of California at Los Angeles, Seattle Children’s Research Institute, and the Boston Children’s Hospital. The Labs of Cognitive Neuroscience worked to recruit, screen, and acquire electrophysiological and behavioral data for individuals in the ACE Network. The focus of this thesis on updating the Kalman detrend step and examining mu suppression in individuals with autism spectrum disorder (ASD) was developed by Dr. C. Nelson, Dr. A. Levin, Professor D. Ba, and A. Acosta. All processing and programming were done in MATLAB R2017a and statistical analyses were performed in SPSS. All figures were created by A. Acosta, except where cited. The structure of this thesis was inspired by M. Shi (2014).

Abstract

When analyzing electroencephalography (EEG) data, noise must be removed from the observed signal in order to parse out the "true" EEG signal. The Kalman detrend step within the Boston EEG Automated Processing Pipeline (BEAPP) removes low-frequency noise from the observed EEG signal. The first part of this thesis develops an update to the Kalman detrend step of BEAPP. This update uses expectation maximization to allow researchers to more accurately and uniquely remove this noise from an observed EEG signal. More rigorous implementation must be done before this new detrend step can be added to BEAPP and used to clean EEG data. The second part of this thesis uses the currently implemented Kalman detrend step within BEAPP to examine mu suppression in individuals with autism spectrum disorder (ASD). In typically developing individuals, females have been shown to display more mu suppression than males when observing human actions. The gender differences in ASD are not well understood and this gender pattern in mu suppression has not been explored in individuals with ASD. Mu suppression was analyzed by comparing the average mu power over the sensorimotor cortex in an eyes closed resting state and when observing the Biological Motion paradigm. The results found no differences in mu suppression between males with ASD and females with ASD.

Contents

0.1	Acknowledgements	1
0.2	List of Contributions	2
I	Boston EEG Automated Processing Pipeline Kalman Detrend Update	4
1	Introduction	5
1.1	Measuring Electrical Activity in the Brain	5
1.2	Introduction to the Boston EEG Automated Processing Pipeline	6
1.3	Introduction to Kalman Processing Step	6
1.4	Current limitations of Kalman Detrend Step and Motivation	8
2	Methods	9
2.1	Materials	9
2.2	Current BEAPP Kalman Detrend Step	9
2.2.1	Kalman Filtering Step	9
2.2.2	Kalman Smoothing Step	13
2.2.3	Covariance Step	13
2.3	Updated BEAPP Kalman Processing Step	13
2.3.1	Covariance Step	14
3	Results	15
4	Discussion	17

II	An Examination Mu Suppression	18
5	Introduction	19
5.1	Autism Spectrum Disorder and Diagnosis	19
5.1.1	Gender Differences in ASD	19
5.2	Relationship between Mu Suppression, Imitation, and the Mirror Neuron System	21
5.3	Mu Suppression in Individuals with ASD	22
5.4	Gender Differences in Mu Suppression in Typically Developing Populations	22
5.5	Biological Motion Task	23
5.6	Motivation	23
6	Methods	24
6.1	Materials	24
6.2	Data Acquisition	24
6.2.1	Participants	25
6.2.2	EEG Recording	25
6.2.3	Cognitive Assessment	26
6.3	EEG Processing	26
6.3.1	Mu Frequency Power Analysis	27
6.4	Statistical Analysis	28
7	Results	29
7.1	Group Characteristics	29
7.2	Mu Suppression in Males with ASD vs. Females with ASD	30
7.3	Relationships between Mu Suppression, Age, and Cognitive Ability	31
8	Discussion	34
8.1	Limitations and Future Studies	35
8.2	Conclusion	37

List of Figures

1	σ_{ϵ}^2 close to zero.	10
2	σ_{ϵ}^2 value close to one.	11
3	Power spectral output as a function of σ_{ϵ}^2	12
4	Updated EEG and trend line.	15
5	Updated detrend output.	16
6	Map of electrodes.	27
7	Mu Power Difference.	30
8	Linear Regression on age.	32
9	Linear Regression on GCA composite.	33

List of Tables

1	Group Statistics.	29
2	Coefficients for Linear Regression.	31

Part I

Boston EEG Automated Processing Pipeline Kalman Detrend Update

Introduction

1.1 Measuring Electrical Activity in the Brain

Exploration of electrical activity in the brain began in the late 1800s with Richard Caton first examining electrical impulses in the brains of animals (Cohen, 1959). More exploration led to the discovery of electroencephalography (EEG) by Hans Berger, a German psychiatrist, in 1929. (Tudor et al., 2005). Over the past 100 years or so, EEG has developed into a common noninvasive method of viewing electrical activity in the brain.

EEGs are useful for diagnosing brain disorders and for the advancement of knowledge on how the brain functions (Binnie et al., 1994). EEGs utilize the electrical response of neurons by measuring postsynaptic potentials (Binnie et al., 1994). These potentials are measured compared to a reference electrode and then amplified and recorded ("Electroencephalogram", n.d.). The signals produced by EEGs are often susceptible to both physical and electrical artifact (Cohen, 1959). There are a variety of factors that can add noise to a signal. There are also a variety of filtering methods that have been used in order to remove noise and artifact (Nitschke, 1998). Ranging from high-pass filtering to visually examining a signal and marking an electrode as damaged, the process of cleaning EEG data varies by researcher and their needs.

1.2 Introduction to the Boston EEG Automated Processing Pipeline

The Boston EEG Automated Processing Pipeline (BEAPP) was created by the Boston Children's Hospital Department of Neurology and the Laboratories of Cognitive Neuroscience to "facilitate the batch process of EEG files for artifact removal and spectral analysis" (Levin et al., 2016). All processes in BEAPP are controlled and determined by the user, but the steps available in BEAPP are as follows: BEAPP begins by using the PREP pipeline created by Bigdely-Shamlo et al. (2015) which uses EEGLab functions created by Delorme et al. (2004) to remove line noise, detect and interpolate bad channels, reference to average while maintaining enough information to allow user to re-reference the data using another method. The user can then filter and resample the data if EEGs being processed have different sampling rates. BEAPP then detrends the data using a mean, linear or Kalman detrend. This detrend step is followed by identifying periods of time which have high-amplitude artifact in any channel. The exact cutoff amplitude is set by the user and these epochs are marked and removed from further analysis. The data can then be referenced to the Laplacian reference or left as average referenced. The data is then segmented into windows of a length set by the user. A windowing type is also set by the user for spectral analysis. The power spectrum is evaluated on each window using MATLAB-based fast fourier transform (fft) or multitaper power spectral density estimate (pmtm). The frequency axis of the power spectrum is interpolated and the results are exported (Levin et al., 2016).

1.3 Introduction to Kalman Processing Step

BEAPP is constantly being updated and improved. One goal of this thesis is to improve the Kalman detrend step within BEAPP. Kalman filters work within a Bayesian framework to use past information to provide means to estimate the state of a process (Welch et al., 2006). Although Kalman filters have a variety of applications, they have been used

previously in EEG data analysis for issues such as removing transcranial magnetic stimulation (TMS) induced artifacts (Morbidi et al., 2007) and removing ballistocardiogram artifacts from EEG signals (In et al., 2006).

In the Labs of Cognitive Neuroscience at the Boston Children's Hospital, the Kalman detrend step is being used to remove the low-frequency noise trend from the EEG signal as part of BEAPP. The Kalman detrend step begins by assuming that x_t is the "true" low-frequency trend, which is the desired noise to be removed. Therefore the observed values, y_t , will be the low frequency noise plus the "true" EEG signal. "True" is put into quotations here because it is impossible to know exactly what the true signals are but these are our best estimates of the true signals. The output x_{t+1} will also be the low-frequency noise added to some smoothness constraint on this noise:

$$y_t = x_t + v_t$$

$$x_{t+1} = x_t + \epsilon_t$$

The signal goes from time $t = 1$ to time $t = T$. All values of v_t and ϵ_t are independent. The values of v_t and ϵ_t are normally distributed so they can be represented as $\mathcal{N}(0, \sigma_v^2)$ and $\mathcal{N}(0, \sigma_\epsilon^2)$ respectively. The Kalman detrend step is therefore designed to make an estimate for x_t by maximizing the likelihood of the estimates given the observed data and estimates of the "true" state (Holmes).

The Kalman detrend step has three parts: filtering, smoothing and a covariance step. The Kalman filtering step takes into account all previous observed EEG values up to a certain point in time to predict the next value in time. The Kalman smoothing step takes into account all observed values of EEG signal when predicting the value at each time step. The covariance step then uses both the filter and the smoother to update the parameters σ_v^2 and σ_ϵ^2 . These new parameters are then used to update the filter and smoother values and the process repeats until the parameter values converge. More details on these steps are given in the Methods section.

1.4 Current limitations of Kalman Detrend Step and Motivation

There are two important parameters when using the Kalman detrend step—an in-depth analysis of how these parameters affect the output of the Kalman detrend step is described in the Methods section. One value entered by the user represents the variance, or the smoothness constraint, on the noise to be removed, or the variance of ϵ_t . The second value represents the variance of the true EEG signal, or the variance of v_t . Both of these values are estimates made by the user. The aim of the first part of this thesis is therefore to improve the Kalman detrend step by updating the initial estimates for these parameters using observed data to make these parameters more accurate using expectation maximum likelihood.

The motivation for updating the Kalman detrend step is to allow the user to more accurately remove noise from the observed signal. This updated Kalman detrend step is a per subject and per electrode mode of removing noise. The Kalman detrend step is used in a variety of EEG research, including in the second part of this thesis. Even with the update demonstrated in the first part of this thesis, there are still improvements that can be made before it is fully added to BEAPP—this will be detailed in the Discussion section. As a result, the updated Kalman detrend step was not used to analyze the data in the second part of this thesis, but in the future it would be beneficial to rerun the data through BEAPP using this new detrend step to more accurately examine the data.

Methods

2.1 Materials

MATLAB R2017a (The Mathworks, Natick, MA)

2.2 Current BEAPP Kalman Detrend Step

As mentioned above, the Kalman detrend step has three main parts: filtering, smoothing, and covariance. The overall goal of the Kalman detrend step is to remove low-frequency noise from the original EEG signal using the observed data and initial guesses for the variances in the true EEG signal and in the smoothness constraint, σ_v^2 and σ_ϵ^2 respectively.

2.2.1 Kalman Filtering Step

The filter is initialized using the observed value at $t = 1$ and runs through all time points until $t = T$. In the data used in the second part of this thesis, the sampling rate was 500 Hz so there is a t value every $\frac{1}{500}$ th of a second.

Prediction Step

At each time step, the filter starts by making a prediction:

$$\begin{aligned}x_{t|t-1} &= x_{t-1|t-1} \\ \sigma_{t|t-1}^2 &= \sigma_{t-1|t-1}^2 + \sigma_\epsilon^2\end{aligned}$$

$x_{t|t-1}$ and $\sigma_{t|t-1}^2$ are first set to some initial value: the first value of the observed EEG signal and one, respectively. In this prediction step, our value for the estimated low-frequency noise at time t is set equal to the previous predicted value at time $t - 1$. Similarly, the variance is set equal to the previous variance with the addition of the smoothness constraint, σ_ϵ^2 .

Importance of σ_ϵ^2

The σ_ϵ^2 value is indirectly set by the user. This is the smoothness constraint and will determine the variance of the low-frequency signal to be removed. So when σ_ϵ^2 is close to zero, the signal to be removed should show very low variance and barely any signal will be removed. Below is a graph of an original EEG signal and the low-frequency signal to be subtracted with a very small value for σ_ϵ^2 .

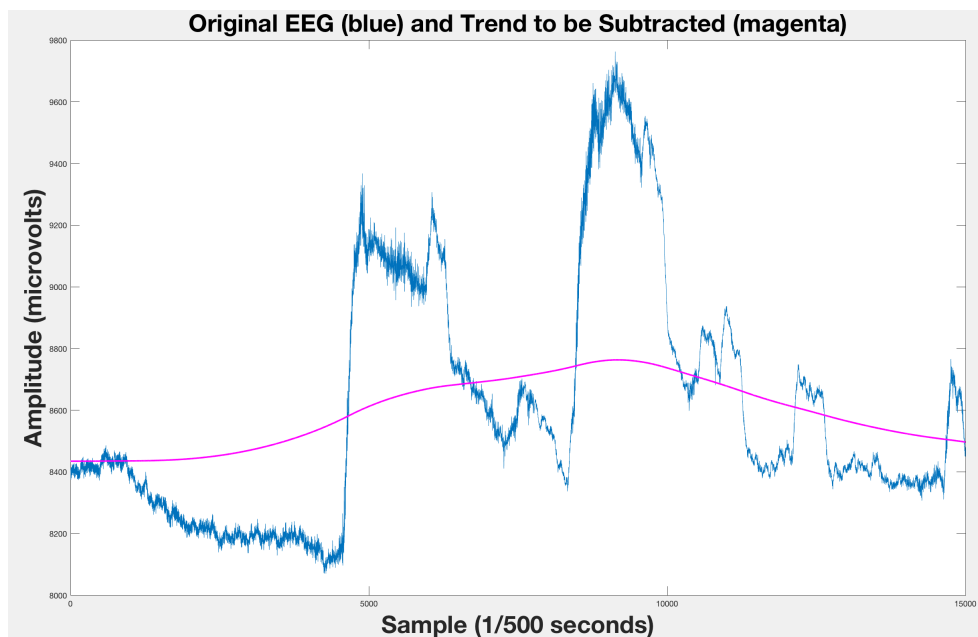


Figure 1: σ_ϵ^2 close to zero.

The graphs above show the original EEG signal in blue over the course of a few seconds. The magenta line shows the trend line to be removed from the original signal. Since the variance of the trend line was set to be close to zero, the variance seen in the magenta line is very small.

In contrast, Figure 2 shows when σ_ϵ^2 is very large meaning a large amount of variance in the low-frequency trend. The original EEG is almost not even visible in this case because it completely overlaps with the trend to be removed.

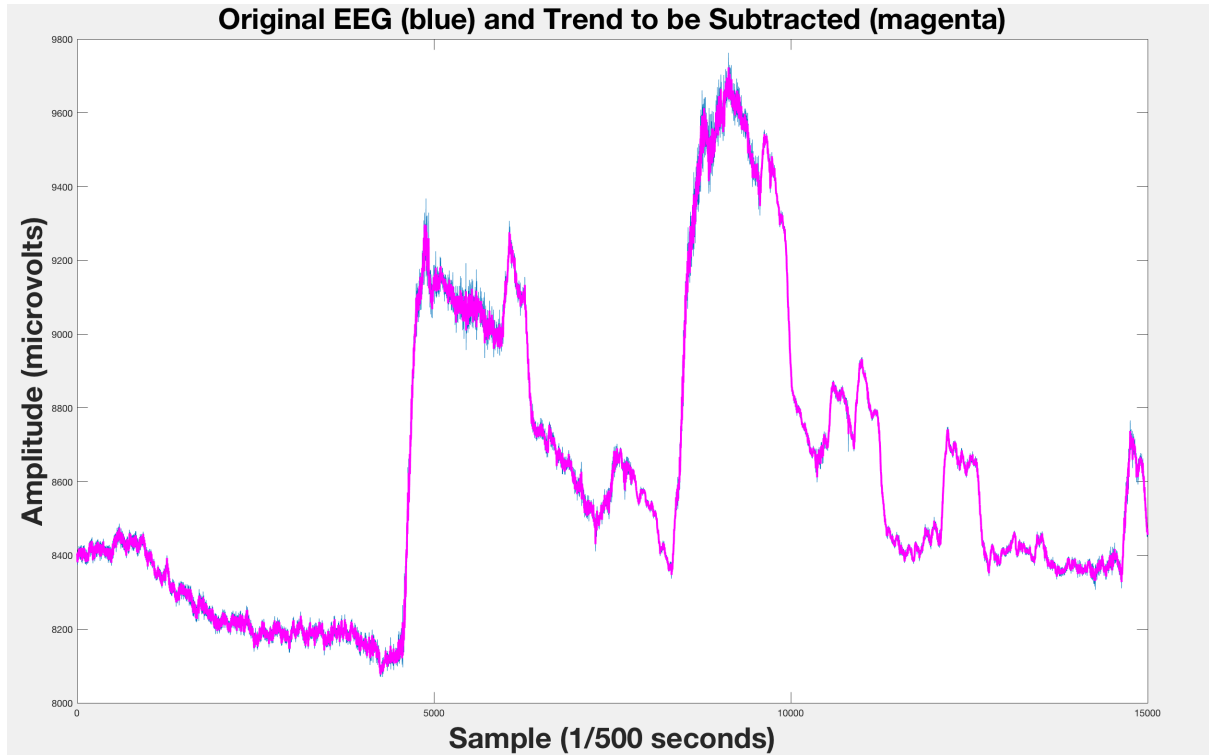


Figure 2: σ_{ϵ}^2 value close to one.

The graph above shows the original EEG signal in blue over the course of a few seconds. The magenta line is the trend to be removed from the original signal. Since σ_{ϵ}^2 was large in this example, the variance of the magenta line is noticeably larger than Figure 1 meaning more signal will be subtracted from the original EEG.

This choice in σ_{ϵ}^2 also affects the power output. For each output signal, a power spectra is created to show the power of each frequency within the signal. In Figure 3, it can be seen that with a lower σ_{ϵ}^2 value, less signal is removed so more signal will be kept. It is important to note that the number of "usable segments" is also affected by σ_{ϵ}^2 . After the signal is run through the Kalman detrend step, any portion of amplitude higher than 150 microvolts is considered high-amplitude artifact and is removed from the zero-crossing point prior to the high amplitude until the zero-crossing point after the high amplitude. Since the Kalman detrend step also brings the mean of the signal down to zero, it is important that the high-artifact removal step comes after the detrend step.

Correction Step

Moving back into how the Kalman detrend function works, the predictions made in the Prediction Step subsection are then updated in a correction step:

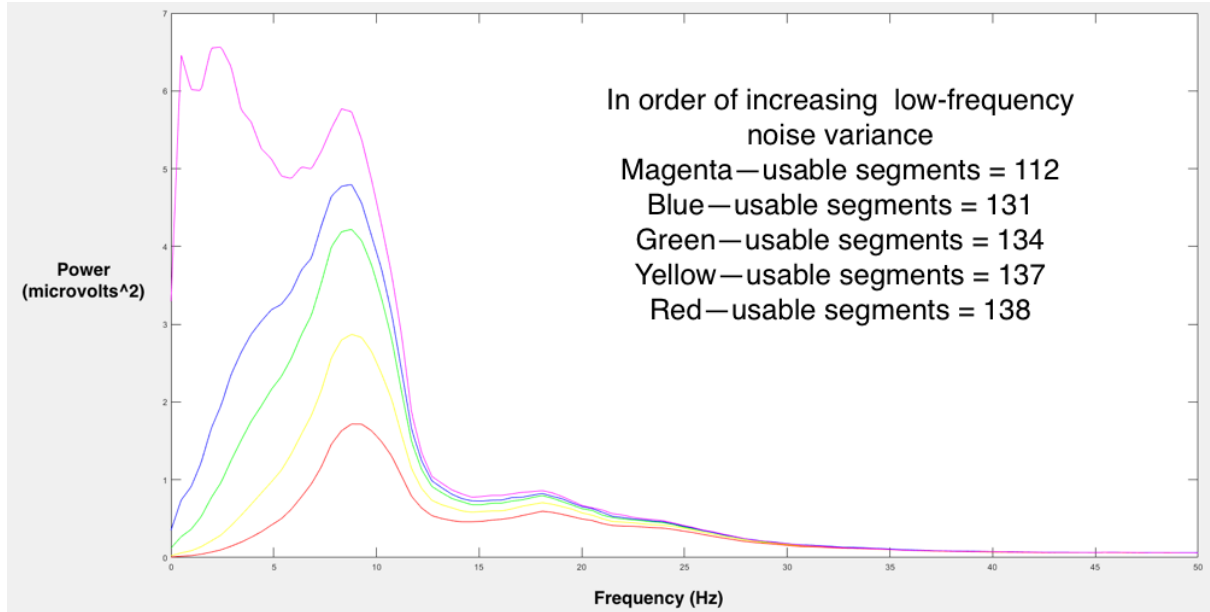


Figure 3: Power spectral output as a function of σ_ϵ^2 .

This graph shows the average power for each frequency for a variety of chosen σ_ϵ^2 values. The smaller the variance, the more data is maintained after the Kalman detrend step, but that also tends to mean more high amplitudes are kept which are removed after the detrend step. Hence, the smallest variance has the smallest number of usable segments.

$$k_t = \frac{\sigma_{t|t-1}^2}{\sigma_v^2 + \sigma_{t|t-1}^2}$$

$$x_{t|t} = x_{t|t-1} + k_t(y_t - x_{t|t-1})$$

$$\sigma_{t|t}^2 = \sigma_{t|t-1}^2 - k_t\sigma_{t|t-1}^2$$

Using the predictions made previously, the correction step then takes the prediction and adjusts it based on the current observed value at time t . k_t is a value that determines how much weight is given to the observed value when making estimates for the low frequency noise signal. Currently the value of one in the denominator is represents σ_v^2 . This value is important for indicating the weight of the observed signal when making the next prediction. For example, if instead of one this value were zero then $x_{t|t}$ would equal y_t meaning the observed signal is entirely low frequency noise. Having σ_v^2 be set to one by default is a limitation of the current Kalman detrend step and will be updated in Section 2.3.

2.2.2 Kalman Smoothing Step

The smoothing step is important as part of the detrend process because it makes predictions about the low frequency signal using all observed values instead of just values up to the point of time in question. This is valuable because it will give a more accurate estimation of the low-frequency trend. The Kalman smoother works backwards starting with time $t = T - 1$ so that it can use the information output by the Kalman filter to start. The smoothing step is written as:

$$b_t = \frac{\sigma_{t|t}^2}{\sigma_{t+1|t}^2}$$
$$x_{t|T} = x_{t|t} + b_t(x_{t+1|T} - x_{t+1|t})$$
$$\sigma_{t|T}^2 = \sigma_{t|t}^2 + b_t^2(\sigma_{t+1|T}^2 - \sigma_{t+1|t}^2)$$

The key note here is that all of these values are given by the Kalman filter, but only if starting at the end of the observed data and working backwards. The outputs to the smoother, $x_{t|T}$ and $\sigma_{t|T}^2$, signify the current best estimate of the low-frequency noise and variance, respectively, using all the observed values.

2.2.3 Covariance Step

The current covariance step in BEAPP is not utilized in the Kalman detrend step, but determines the covariance between σ_t^2 and σ_{t-1}^2 . This step will be utilized in the parameter update described in the next section.

2.3 Updated BEAPP Kalman Processing Step

In this updated format, parameters which the user can enter are now being used as initial guesses of the variance of the true EEG signal and low-frequency smoothing constraint. The covariance step now updates the values for σ_e^2 and σ_v^2 . The new function runs the detrend step repeatedly until the values for σ_e^2 and σ_v^2 converge instead of just using initial guesses for the entire detrend step.

2.3.1 Covariance Step

The update to the function comes in the covariance step. The goal is to maximize the log of the probability of seeing the observed values, y_t , and the low frequency estimate, x_t , when given initial guesses for the variances, $\sigma_v^2(0)$ and $\sigma_\epsilon^2(0)$.

Maximize: $E[\log P(y_t, x_t | y_t, \sigma_v^2(0), \sigma_\epsilon^2(0))]$ Let $y_t, \sigma_v^2(0), \sigma_\epsilon^2(0) = \theta$

$$E\left[-\frac{1}{2\sigma_v^2} \sum_{t=1}^T (y_t - x_{t|T})^2 - \frac{1}{2\sigma_\epsilon^2} \sum_{t=1}^T (x_{t|T} - x_{t-1|T})^2 | \theta\right]$$

We can derive:

$$\sigma_v^2 = \frac{1}{T} \sum_{t=1}^T E[(y_t - x_{t|T})^2 | \theta]$$

$$\sigma_v^2 = \frac{1}{T} \sum_{t=1}^T y_t^2 + E[x(t)^2 | \theta] - 2y_t E[x_{t|T} | \theta]$$

And:

$$\sigma_\epsilon^2 = \frac{1}{T} \sum_{t=1}^T E[(x_{t|T} - x_{t-1|T})^2 | \theta]$$

$$\sigma_\epsilon^2 = \frac{1}{T} E[x_{t|T}^2 | \theta] - 2E[x_{t|T} x_{t-1|T} | \theta] + E[x_{t-1|T}^2 | \theta]$$

The final covariance parameter updates are therefore:

$$\sigma_v^2(l) = \frac{1}{T} \sum_{t=1}^T y_t^2 + \sigma_{t|T}^2 + x_{t|T}^2 - 2y_t x_{t|T}$$

$$\sigma_\epsilon^2(l) = \frac{1}{T} \sum_{t=1}^T \sigma_{t|T}^2 + x_{t|T}^2 - 2(\sigma_{t|T}^2 \frac{v_{t-1|t-1}^2}{\sigma_{t|t-1}^2} + x_{t|T} x_{t-1|T}) + \sigma_{t-1|T}^2 + x_{t-1|T}^2$$

To check for convergence, the difference between the new likelihood value and the previous likelihood value is determined and if the difference is less than some small threshold, then one can say that the log likelihood converges (Holmes).

Results

Using code from Holmes, which was an extension of Shumway and Stoffer (1982), we were able to create a detrend step which appropriately determines σ_v^2 and σ_ϵ^2 values on a per subject basis. Below is a zoomed-in, one second sample of original EEG data in blue and the trend to be subtracted—the low-frequency noise—in magenta.

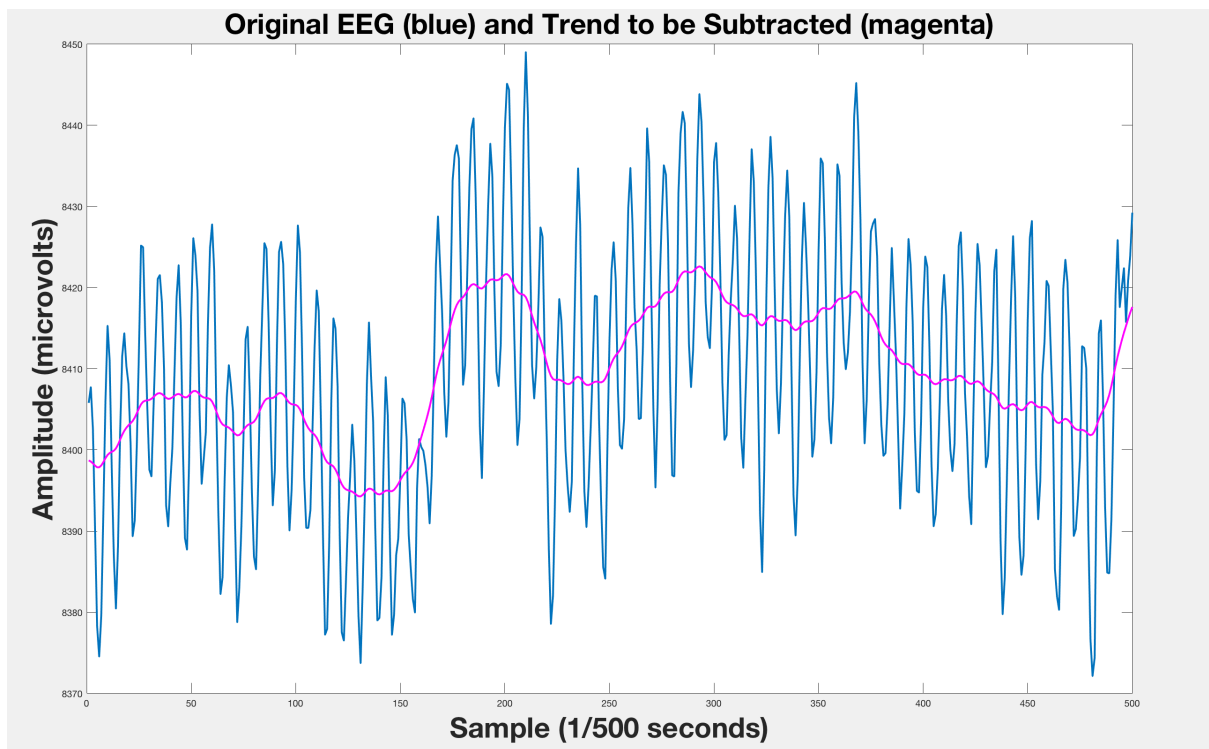


Figure 4: Updated EEG and trend line.

The graphs above are a close up on a one second segment of original EEG signal in blue and the trend to be removed in magenta.

It can be seen here that the trend line is removing low frequency trends. Below is a figure of the resulting signal after the trend has been subtracted. This graph is our estimated "true" EEG signal. Notice that the graph now has a mean of zero and the

difference in amplitude is closer to 60 microvolts, an appropriate and expected EEG signal.

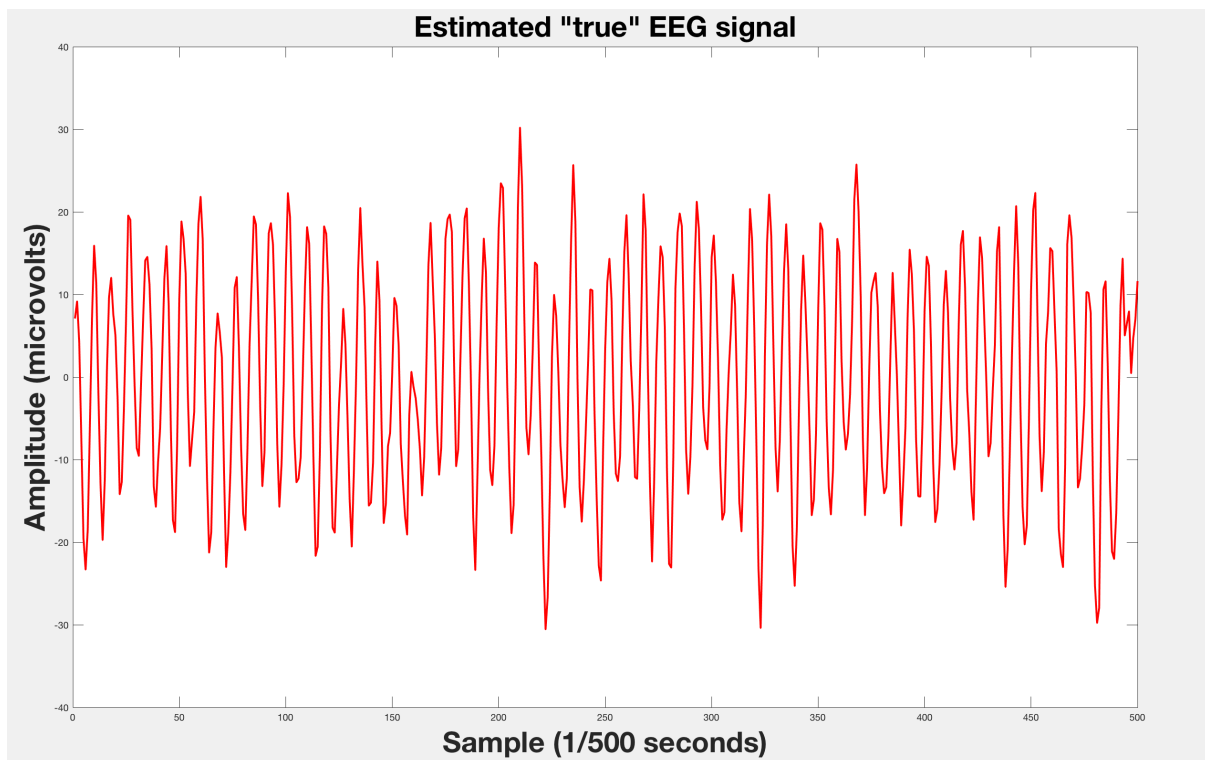


Figure 5: Updated detrend output.

This graph shows the estimated "true" EEG signal. It is determined by subtracting the trend line from the original EEG signal. It is important to note that this signal has a mean of 0 and desired amplitudes for what is expected of an EEG signal.

Discussion

Measuring electrical activity in the brain has given useful insight into the brain for scientists since its discovery in the late 1800s (Cohen, 1959). In measuring electrical activity, however, researchers must be cognizant of the noise included when acquiring a signal. Whether that be from physical movement, power lines, or the equipment itself, this noise does not accurately represent the electrical activity in the brain. The Kalman detrend step used in BEAPP is designed to remove low-frequency noise from EEG signals by making a best estimate for the noise trend using observed data. The detrend step currently uses only the estimated guesses produced by the user for the "true" EEG noise variance and the variance of the trend to be removed. This update involved using expectation maximization to determine a more accurate mode of filtering out low-frequency noise. Through this update, unique parameters were determined for σ_ϵ^2 and σ_v^2 for each signal. The next step in fully implementing this new Kalman detrend step for BEAPP is to use data to make the initial estimates instead of having the user make these estimates. This implementation would impact researchers using BEAPP and allow users to analyze more accurate estimates of the "true" EEG signal. The next section will use the existing Kalman detrend step in BEAPP to analyze EEG data while examining mu suppression. Without this Kalman detrend step in general, the signal would be too noisy to analyze, however the update described here would make the signal even more accurate. In moving forward, it would be beneficial to also re-analyze the mu suppression data after processing it through the new Kalman detrend step.

Part II

An Examination Mu Suppression

Introduction

5.1 Autism Spectrum Disorder and Diagnosis

Autism Spectrum Disorder (ASD) is characterized by difficulties in social communication and restricted, repetitive behaviors. (American Psychiatric Association, 2013). A diagnosis typically includes a developmental screening and if the child appears at risk for ASD, it is followed up by a comprehensive diagnostic evaluation (Christensen et al., 2016). Since ASD is currently characterized solely by behavior, most children are not diagnosed until about four years of age on average (Christensen et al., 2016).

Difficulty in imitation is a characteristic often associated with ASD (Bernier et al., 2007). Children with ASD have shown significantly poorer performance on motor imitation tasks compared to typically developing children (Jones et al., 1985). Adults with ASD have similarly shown significantly poorer performance in imitation ability compared to typically developing adults (Bernier et al, 2007). Mu suppression is thought to be one correlate for quantifying an individual's ability to imitate. In this thesis, mu suppression is analyzed as one way to potentially examine the ability to imitate in males and females with ASD.

5.1.1 Gender Differences in ASD

ASD is far more prevalent in males than in females with a ratio of about 4.3:1 (Fombonne, 2005). The reason for this gender imbalance is still unknown, and research on this topic has been difficult because it is challenging to obtain a significant sample size of females

with ASD. Studies exploring gender differences in ASD have also sometimes been shown to give conflicting evidence or no differences between genders at all. Tsai et al. (1983) found that boys had greater receptive and expressive language abilities than girls with ASD. Carter et al. (2007) similarly found girls with ASD had greater communication impairments than boys with ASD. However, Holtmann et al. (2007) found no significant gender differences in communication abilities. Both the Holtmann et al. (2007) study and the Carter et al. (2007) study used the Autism Diagnostic Observation Schedule (ADOS) as one of their measures for examining communication abilities, but both had different results. A potential reason for this is that the Holtmann et al. (2007) study examined individuals with a mean age of 11 years and 9 months while the Carter et al. (2007) study examined toddlers with a mean age of 28 months. The Tsai et al. (1983) study also examined children with ASD. It is possible that as individuals with ASD get older they are able to improve their communication abilities. The Holtman et al. (2007) study also examined equal numbers of males and females with ASD that were matched for age and IQ unlike Carter et al. (2007) and Tsai et al. (1985). It is therefore possible that any gender differences seen in Carter et al. (2007) and Tsai et al. (1985) were due to the skewed sample sizes. A few studies have shown lower IQ scores in females with ASD such as Nicholas et al. (2008) which found that 72.7 percent of females had IQs below 70 while only 56.4 percent of males had IQs below 70. Banach et al. (2009) similarly found lower IQ scores in females with ASD than males with ASD. Generally, studies have shown no differences in restricted and repetitive behaviors between males and females with ASD (Banach et al. 2009, Carter et al. 2007, McLennan et al. 1993, Holtmann et al. 2007). Carter et al. (2007) found males had better gross motor skills than females with ASD. The current findings are not satisfying for understanding why this gender ratio in ASD may exist and this thesis aims to continue to explore this question.

5.2 Relationship between Mu Suppression, Imitation, and the Mirror Neuron System

Mu waves are seen on the scalp overlying the motor cortex. When performing an action or when seeing an action performed, these waves are suppressed (Pineda et al., 2000). Mu waves are typically thought of as around 8-13 Hz and very low mu waves have been seen in infants as young as 6 months old (Berchicci et al., 2011). The frequencies of mu waves have been shown to increase significantly between the ages of 11 weeks and 47 weeks (Berchicci et al., 2011). If a subject shows mu suppression when viewing someone else perform an action, then the subject's brain is responding as if the subject were performing that action.

The mirror neuron system is a system of neurons in the premotor cortex that fire not only when performing an action, but also when observing an action (Di Pellegrino et al., 1992). In humans, this response of the premotor cortex has been shown through mu suppression, MEG, and TMS (Rizzolatti et al., 2004). The mirror neuron system is therefore thought to be a neurobiological mechanism for mu suppression.

Mu suppression and the mirror neuron system are also shown to relate to ability to imitate. Molenberghs et al. (2009) showed that mirror neurons are involved in imitation by using a meta-analysis of published functional Magnetic Resonance Imaging (fMRI) studies that examined the role of frontal and parietal regions of the brain in imitation. Studies have also shown a relationship between mu suppression and imitation abilities. Specifically, Bernier et al. (2007) found that individuals with ASD showed significantly less mu suppression than typically developing individuals and that imitation skills were correlated with the strength of mu suppression while observing an action.

The relationship between mu suppression, the mirror neuron system and imitation is important when discussing ASD because generally children with ASD perform worse on imitative tasks (Williams et al., 2004). In examining gender differences in mu suppression in ASD, the hope of this thesis is also explore how mirror neurons and imitation abilities may be different or similar between genders.

5.3 Mu Suppression in Individuals with ASD

Although the research on mu suppression and ASD is continually expanding, studies generally show less mu suppression in ASD populations compared to typically developing populations. Martineau et al. (2008) found that typically developing 5-7 year old children showed mu suppression during observation of a human action, but 5-7 year old children with ASD did not. Oberman et al. (2005) found that individuals with ASD showed significantly less mu suppression when observing a hand movement relative to typically developing individuals. Oberman et al. (2013) combined data from multiple studies to examine 66 individuals with ASD and 51 typically developing individuals. This sample size is much larger than most studies and they found a significant difference between typically developing individuals and individuals with ASD in mu suppression in 6-17 year olds when observing an action. Typically developing individuals showed more mu suppression. However, Raymaekers et al. (2009) found no difference in mu suppression between individuals with ASD and typically developing individuals. One reason for the difference in results may be that Raymaekers et al. (2009) specifically examined children with high functioning ASD meaning they may have stronger imitation skills compared to other children with ASD. One study found that mu suppression in individuals with ASD was stronger when observing someone familiar to them perform an action than watching a stranger perform an action (Oberman et al., 2008).

5.4 Gender Differences in Mu Suppression in Typically Developing Populations

Yang et al. (2008) found that adult females showed stronger mu suppression than males when watching both painful and non-painful situations. Some of these same researchers did a similar study by having typically developing subjects watch either hand actions or a moving dot and they found, again, that females showed significantly stronger mu suppression than males when watching hand actions (Cheng et al., 2008). This difference

in genders, however, has not been explored in individuals with ASD and is the main question behind this portion of the thesis.

5.5 Biological Motion Task

The Biological Motion task was examined in this study. The task has two stimuli both created using point-light animations. One stimuli is of coherent biological motion made by an adult male actor performing movements relevant to children. The other is scrambled motion animation. The biological motion portions are intended to and have been shown to elicit mu suppression. Saygin et al. (2004) found activation of the premotor cortex in response to point-light biological motion. Ulloa et al. (2007) similarly found that point-light biological motion stimuli produced mu suppression relative to baseline. However, it is important to note that Klin et al. (2009) found that infants with ASD failed to recognize biological motion. Blake et al. (2003) similarly found that children with ASD had significant impairment in recognizing biological motion. The limitations of this will be addressed in the Discussion section.

5.6 Motivation

Since most research on ASD is skewed towards males due to the 4:1 gender ratio, it is important to explore gender differences in mu suppression in individuals with ASD to help determine if treatment and diagnosis for females is appropriate. Further, exploring mu suppression between genders with ASD could also give insight into differences or similarities in the functioning of the mirror neuron system.

Knowing that there is a difference in mu suppression between genders in typically developing population, I hypothesized that there would be a difference in mu suppression between males and females with ASD as well. Knowing that the ratio of males to females with ASD is about 4:1 and that differences in mu suppression are seen in typically developing individuals, then examining mu suppression in individuals with ASD seems like a logical place to look for gender differences.

Methods

6.1 Materials

128-Channel HydroCel Geodesic Sensor Net (Electrical Geodesics Inc., Eugene, OR)

NetStation (Electrical Geodesics Inc., Eugene, OR)

MATLAB R2017a (The Mathworks, Natick, MA)

SPSS (IBM Software)

Differential Ability Scale (DAS-II) (Pearson Education, Inc.)

6.2 Data Acquisition

The data used in this study was collected as part of the Autism Center of Excellence (ACE Network). The researchers involved in the ACE Network include Yale University, University of California at Los Angeles, Seattle Children's Research Institute, and the Boston Children's Hospital. The data was obtained only from the Boston Children's Hospital. One of the goals of the ACE Network is to examine gender differences in brain structure, function, connectivity in children and adolescents with ASD and to relate these differences to differences behavior and genetics.

6.2.1 Participants

The total sample is expected to include 625 8-17 year olds: 125 females with ASD, 125 typically developing females, 125 males with ASD, 125 typically developing males, and 125 unaffected siblings (63 female and 62 male). This thesis analyzed 20 males with ASD and 10 females with ASD. According to the protocol, all participants had 20-20 (corrected or uncorrected) vision. Potential participants were screened for active psychiatric disorders other than ASD using the Child/Adolescent Symptom Inventory 4—a checklist designed to screen for DSM-IV disorders in children and adolescents. Individuals with ASD were excluded if they had a twin, were pregnant, suffered from seizures or another neurological disease, had a history of serious head injury, had sensory or motor impairment or current psychiatric illness that would prevent completion of study protocol, or if they were taking medication known to affect brain electrophysiology or BOLD signal. Subjects also had an IQ greater than 70. Written consent was obtained from the parents or guardians of children and children were given age-appropriate assent forms before participating in the study.

6.2.2 EEG Recording

The ACE Network aims to collect data from a variety of experiments in addition to collecting a blood sample to examine genetics. This study looked specifically at existing Biological Motion and eyes closed resting data collected using EEG in the Boston Children’s Hospital’s Labs of Cognitive Neuroscience. EEG data was collected using 128 channel Hydrocel Sensor Nets (EGI, Eugene, OR) with time-locked video of the participant. Data was collected using EGI NetAmps 300 and NetStation with a sampling rate of 500 Hz. The exact net used is based on the head size of the subject. Nets are soaked in a warm solution of water, KCl and baby shampoo before they are placed on the subject’s head. Throughout the EEG collection process, the subject is seated in a dark recording room facing a screen.

As noted in the Introduction, the Biological Motion task has two stimuli both created

using point-light animations. One stimuli is of coherent biological motion made by an adult male actor performing movements relevant to children and the other is scrambled motion animations. Resting data was collected by having participants watch a short video and having participants sit with their eyes closed for a few minutes. Only eyes closed resting data was used in this analysis.

6.2.3 Cognitive Assessment

The Differential Ability Scale (DAS-II) (Pearson Education, Inc.) was used to assess cognitive ability. The test is designed to measure verbal, nonverbal reasoning, and spatial reasoning abilities. It was used in this analysis to account for differences in cognitive function when examining mu suppression. Specifically, the General Conceptual Ability (GCA) Composite score was used.

6.3 EEG Processing

The data was first exported from NetStation to MATLAB using a NetStation waveform tool. As introduced above, the Boston Children’s Hospital’s Labs of Cognitive Neuroscience uses BEAPP for the cleaning of EEG data. BEAPP was used here to run the data through PREP, remove low-frequency using a Kalman detrend with a b value of 0.999, and to remove data with amplitudes above 150 microvolts. Once the updated Kalman detrend step from Part I is fully implemented, it would be used here to detrend the data. BEAPP then cut the data into two second segments for multitaper windows with three tapers for power spectrum calculations. A b value of 0.999 is the same as a 0.001 value for σ_ϵ^2 described in Part I meaning a pretty low variance for the trend to be removed. This b value was chosen because $b = 0.999$ was shown to maintain a large amount of usable data, specifically in the frequencies of interest (8-13Hz), while still appropriately removing noise. As noted in Part I, with the future implementation of the Kalman detrend step, the b value entered by the user would simply be the first estimate and the function would determine a more accurate b value.

6.3.1 Mu Frequency Power Analysis

The mu frequency band is accepted to be around 8-13 Hz. This range was also examined in the Cheng et al. (2008) and Yang et al. (2008) which were the inspiration for this study. Mu suppression is generally viewed over the sensorimotor cortex which corresponds to electrodes 36 (C3) and 104 (C4) in the 128-Channel HydroCel Geodesic Sensor Net. These electrodes are boxed-in in Figure 6.

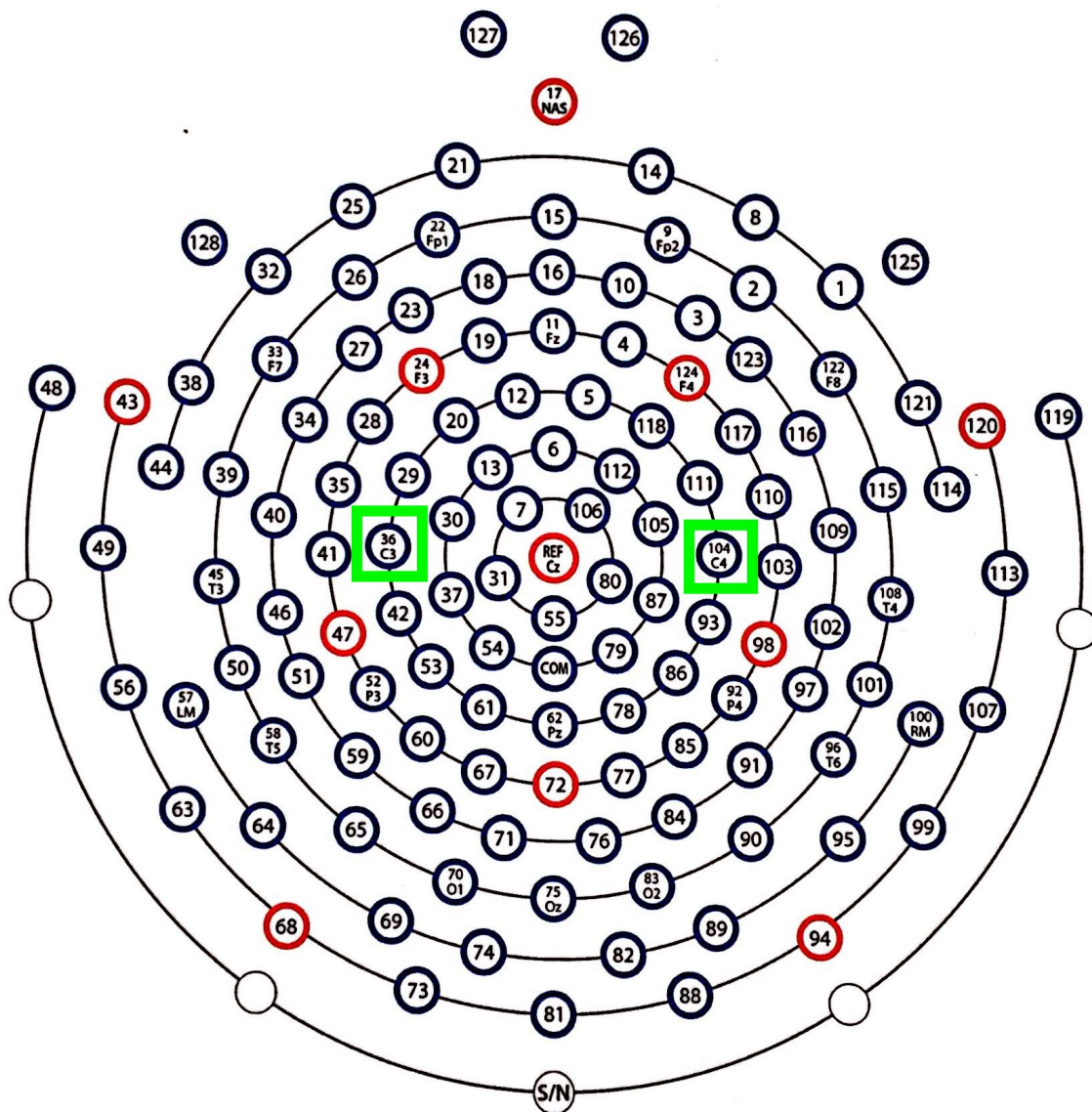


Figure 6: Map of electrodes.

This is a map of electrodes for a 128-Channel HydroCel Geodesic Sensor Nets provided by Electrical Geodesics Inc. (Eugene, OR)

To begin, the average power over C3 and C4 in the 8-13 Hz band was computed for each

individual for all eyes closed trials—meaning the portions of time during which resting data was collected while the subject had their eyes closed—and for the entire biological motion portion of the data using the power spectra output by BEAPP. It is important to note that the Biological Motion portion examined here included both biological motion and scrambled animation with the intent that overall a net mu suppression would be expected—more on how this could be improved for future studies is detailed in the Discussion section. All of these values were then placed in an informational table along with age, gender, and cognitive ability. Mu suppression was then calculated by subtracting the Biological Motion mu power from the eyes closed mu power. This was the method used to analyze mu suppression by Yang et al. (2008) which was one of the the inspirations for this part of the thesis. Mu suppression was also analyzed by checking the value of $\log\left(\frac{\text{BiologicalMotionMuPower}}{\text{RestingMuPower}}\right)$ because this has been done in other papers examining mu suppression such as Bernier et al. (2013). The results of both analyses were the same so only the analysis of difference in mu power values will be shown.

6.4 Statistical Analysis

Statistical analyses were conducted in SPSS. Any subject with less than ten usable segments of data for Biological Motion or Eyes Closed data was rejected. In the final analysis, 12 males were analyzed and 8 females. The EEG data was not normally distributed based on a Shapiro-Wilk ($p < 0.05$) and histogram observation. Therefore, Mann-Whitney U nonparametric tests were used to compare mu suppression between males and females. Linear regressions were also run to examine relationships between mu suppression, age, and cognitive abilities.

Results

7.1 Group Characteristics

The characteristics of each group can be seen in Table 1.

Group Statistics					
	Sex	N	Mean	Std. Deviation	Std. Error Mean
Age	Male	12	13.0070	3.18653	.91987
	Female	8	11.8018	3.25084	1.14934
Total Biological Motion Segments	Male	12	108.50	25.742	7.431
	Female	8	110.25	33.847	11.967
Total Eyes Closed Segments	Male	12	27.75	7.794	2.250
	Female	8	23.63	7.269	2.570
GCA Composite Score	Male	12	89.0000	13.10794	3.78394
	Female	8	104.5000	30.45371	10.76701

Table 1: Group Statistics.

Males with ASD and females with ASD were found to be similar across number of segments studied, age, and cognitive ability.

An Independent Samples T-test was used to examine between group differences because all age, segment, and GCA composite values were normally distributed. The differences in means between groups failed to reject the null hypothesis, suggesting that groups were similar in age, cognitive abilities, and total data analyzed.

7.2 Mu Suppression in Males with ASD vs. Females with ASD

Overall, The Mann-Whitney U nonparametric test revealed no significant differences in mu suppression between males with ASD and females with ASD. The mu suppression boxplot for both genders can be seen in Figure 7.

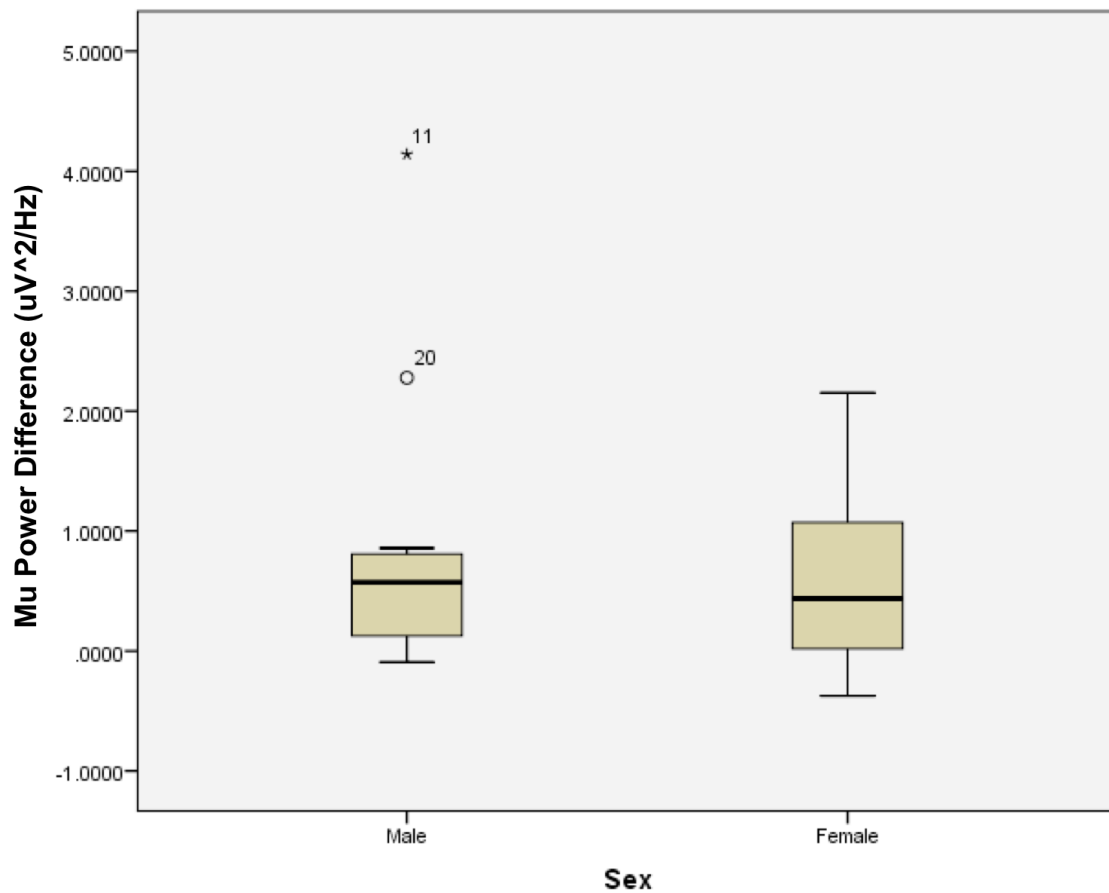


Figure 7: Mu Power Difference.

The graph shows the minimum, first quartile, median, third quartile, and maximum mu power differences between Biological Motion and resting values for male with ASD and females with ASD.

7.3 Relationships between Mu Suppression, Age, and Cognitive Ability

The relationship between mu suppression, age, gender, and cognitive ability was explored using a linear regression. The results of the linear regression can be seen in Table 2. This linear regression showed no significant correlations between mu suppression, age, gender and cognitive ability.

Coefficients ^a						
Model		Unstandardized Coefficients		Standardized Coefficients	t	Sig.
		B	Std. Error	Beta		
1	(Constant)	2.400	1.566		1.533	.145
	Sex	-.198	.541	-.095	-.365	.720
	Age	-.059	.081	-.179	-.729	.477
	GCA Composite Score	-.009	.012	-.186	-.722	.481

a. Dependent Variable: Mu Suppression Power Difference

Table 2: Coefficients for Linear Regression.

A linear regression was examined to check for correlations between sex, age, or cognitive ability and mu suppression. No statistically significant correlations were found.

The regression line between Mu Power Difference and age as well as between Mu Power Difference and GCA composite score can be seen below and, again, the correlations were shown to lack statistical significance.

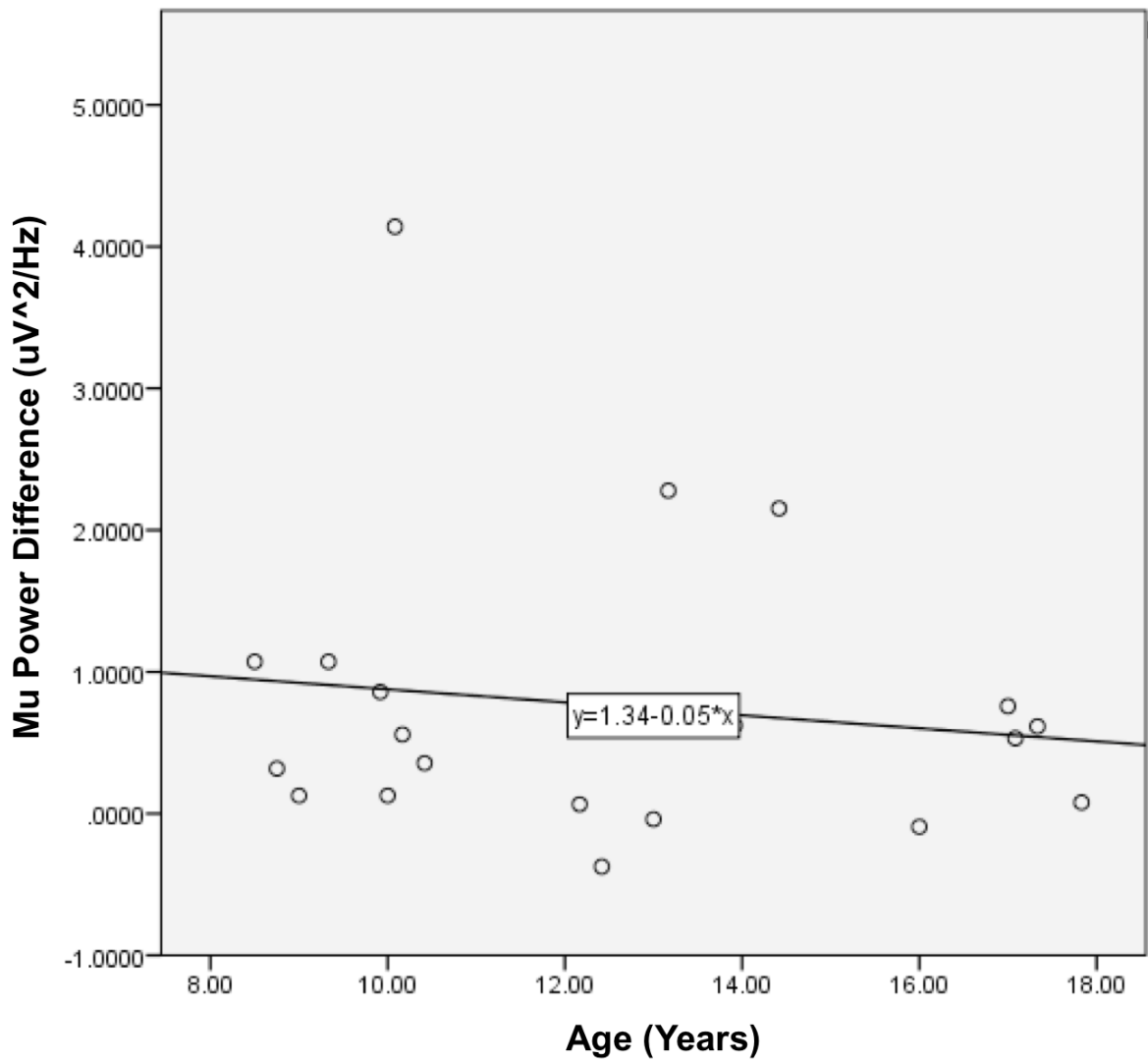


Figure 8: Linear Regression on age.
No significant correlation between age and mu suppression was found.

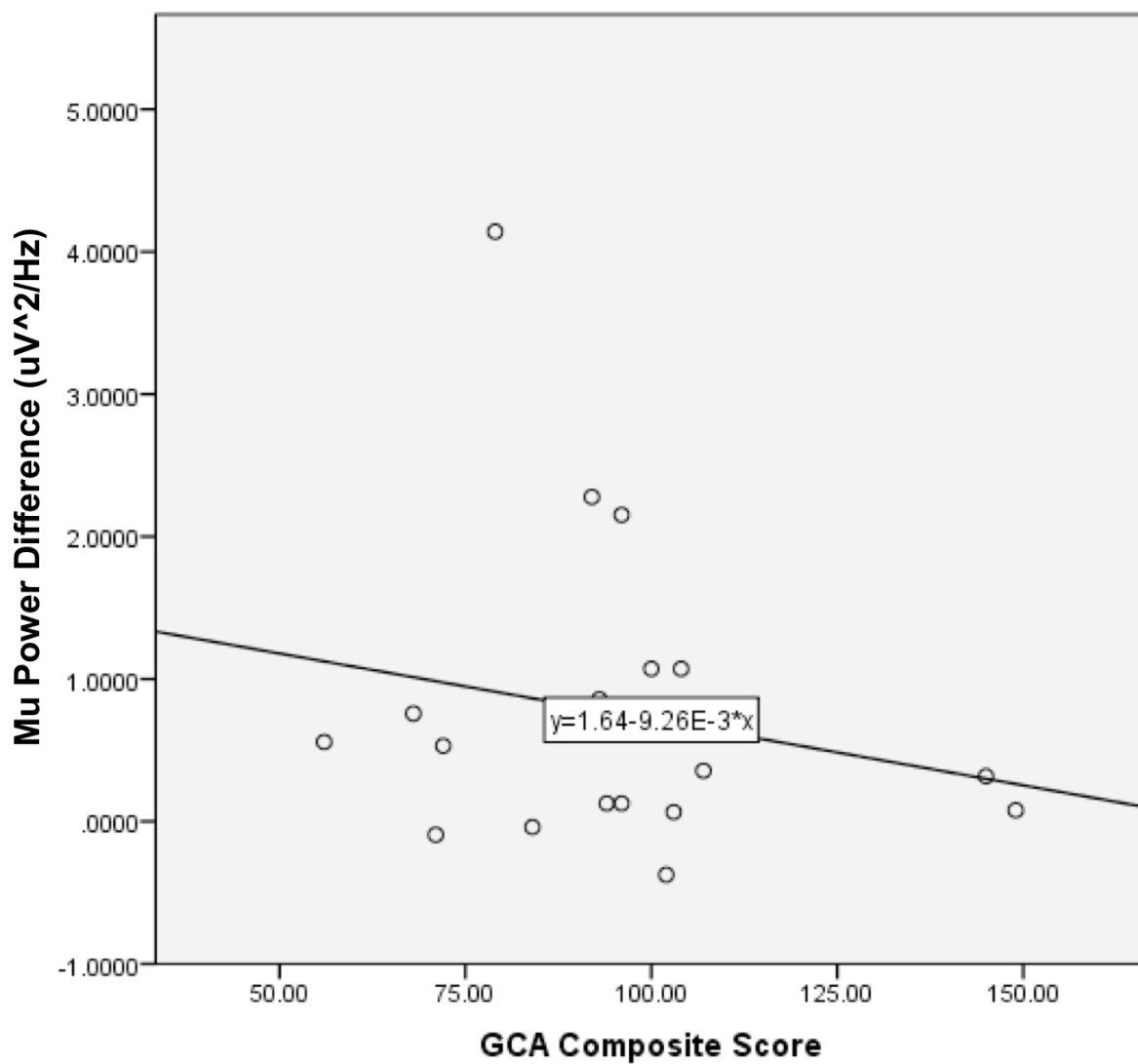


Figure 9: Linear Regression on GCA composite.
 No significant correlation between cognitive ability and mu suppression was found.

Discussion

The lack of a significant difference in mu suppression between males with ASD and females with ASD was not hypothesized, and the lack of a difference can be attested to a few factors. Since no differences in mu suppression were seen, this would suggest that males and females with ASD may have similar mirror neuron abilities. This finding along with other findings that show no differences between males and females with ASD suggest that there may be a different reason for the gender ratio difference.

It is important to note here that it is possible that males and females that are diagnosed with ASD may have similar mirror neuron functioning, but there may be females with deficits masked by the ability to imitate that are not diagnosed with ASD. Meaning there may be females that suffer from the same challenges as individuals with ASD, but are not diagnosed due to their ability to imitate. One suggestion for the difference in gender prevalence is that females with ASD may be better able to imitate those around them, making it more difficult to behaviorally see deeper social/cognitive deficits (Kopp et al., 1992). Knowing that mu suppression is often a correlate for ability to imitate and that individuals with ASD generally have trouble with imitation, a female diagnosed with ASD would be expected to show significant symptoms before being diagnosed and therefore it is possible that in this study, and in other studies examining females with ASD, only the extreme cases are being analyzed. A female with a strong ability to imitate but deeper social deficits would be expected to show higher mu suppression than an individual with ASD that lacks the ability to imitate, but that female may not be diagnosed with ASD.

8.1 Limitations and Future Studies

The lack of a significant difference in mu suppression between groups could also be due to limitations within the study. One limitation is the use of Biological Motion as an indicator of mu suppression. Although point-light biological motion has been shown to elicit mu suppression in typically developing populations (Ulloa et al., 2007), as mentioned previously, it has been seen that children with ASD can have trouble recognizing light-point biological motion as a person moving (Blake et al. (2003), Klin et al. (2009). The inability to recognize the animation as biological motion may have more to do with pathways involving the recognition of human movement as opposed to ability to imitate therefore making Biological Motion a less than ideal mode of analyzing mu suppression. There are a few ways to move forward from this limitation depending on what one is looking for. To examine differences involving recognition of human movement between males and females, one could do a task similar to that done in the Blake et al. (2003) study which involved having the child verbally say whether they thought the animation was "a person" or "not a person." This task would localize the question of whether or not the child is able to interpret the biological motion portion as a person moving. To continue to explore mu suppression gender differences, it would be best to have the stimuli be a clear in-person action. For example, the task could involve having a research assistant do jumping jacks inside of the research room. It would be beneficial to look at the differences between typically developing subjects and subjects with ASD in this study as well. This would be valuable for two main reasons. One, would be to see if a gender difference in mu suppression is seen in typically developing individuals. The Yang et al. (2008) study examined adults, so if a pattern is not seen among younger typically developing individuals, perhaps mu suppression is not a good route of exploration in search of gender differences. Two, to compare individuals with ASD to typically developing individuals because we would expect to see less mu suppression in individuals with ASD (Martineau et al, 2008, Oberman et al, 2005, Oberman et al, 2013).

The Biological Motion section examined here included both the biological motion

animations and the scrambled animations. The current processing tools limited my ability to separate out these two parts efficiently. Studies have shown that in typically developing populations, subjects show less mu suppression when observing scrambled point-light animations (Ulloa et al., 2007). Therefore, even if a subject were eliciting mu suppression during the biological motion portions, the results would be diluted in combination with a potential lack of mu suppression in the scrambled segments. Future studies should examine both of these stimuli separately to compare the three states of resting, scrambled animation, and biological motion. Exploring the difference in mu suppression between scrambled animation and resting data and the difference between biological motion and resting data could also give insight into an individual's ability to distinguish between human movement and random dots.

It is important to note that in any future study it would be important to analyze both typically developing males and females along with males and females with ASD. Although the Yang et al. (2008) paper showed more mu suppression in typically developing females than in typically developing males, this study was done in adults. It would be interesting to see if, first of all, this pattern exists in adolescents, and second, if there are mu suppression differences between all four groups. For the future, I would recommend a study that has a larger sample size of closer to 50 of each group, but of the same age range of interest. There would be four groups including typically developing males, typically developing females, males with ASD and females with ASD. The study would analyze both mu suppression and ability to imitate in order to test if the relationship between mu suppression and ability to imitate. To elicit mu suppression, I would recommend having a familiar person (such as mom or dad) do jumping jacks. The reason for having a familiar person do the jumping jacks is based on Oberman et al. (2008) which found individuals with ASD should stronger mu suppression when observing someone familiar to them perform an action than when observing a stranger. Imitation skills would be scored based on the Mature Imitation Task used by Bernier et al. (2007). I would also use the updated Kalman detrend step to detrend the data. The relationship between mu suppression and imitation ability would then be examined and differences between

groups could be determined.

8.2 Conclusion

Typically developing females have shown more mu suppression when observing a human action relative to typically developing males (Yang et al., 2008), however, this pattern has not been specifically studied in individuals with ASD until this thesis. Since, ASD is significantly more prevalent in males than females (Fombonne, 2005), differences between males and females with ASD is continually being examined and this study aimed to explore mu suppression differences between males and females with ASD. The difference between mu power in eyes closed resting trials and Biological Motion trials was compared between males with ASD and females with ASD. No significant differences were found between groups and no correlations were found between mu suppression and age, gender, or cognitive abilities. These results suggest similar mirror neuron function between males and females diagnosed with ASD, but lead to more questions. It is possible that the females diagnosed with ASD are more likely to have mirror neuron impairments that cause imitation deficits, while females without mirror neuron impairments may have similar deficits to individuals with ASD but are not diagnosed (Kopp et al., 1992). Or that females and males with ASD do in fact have similar mirror neuron functionality and the difference in the gender ratio may due to other factors. On a more practical note, since males and females with ASD were shown to have similar levels of mu suppression in this study, it can be inferred that treatment focusing on imitation abilities may be beneficial for males and females with ASD. More rigorous and widespread research on gender differences in ASD should be done to ensure that both males and females with ASD are receiving appropriate diagnoses and treatments and to help in the longterm search for mechanisms behind the gender differences in ASD.

Bibliography

- [1] American Psychiatric Association. (2013). *Diagnostic and Statistical Manual of Mental Disorders*, 5th Edition. Arlington, VA: American Psychiatric Publishing, Inc.
- [2] Banach, R., Thompson, A., Szatmari, P., Goldberg, J., Tuff, L., Zwaigenbaum, L., and Mahoney, W. (2009). Brief report: Relationship between non-verbal IQ and gender in autism. *Journal of Autism and Developmental Disorders*, 39(1), 188.
- [3] Berchicci, M., Zhang, T., Romero, L., Peters, A., Annett, R., Teuscher, U., ... and Comani, S. (2011). Development of mu rhythm in infants and preschool children. *Developmental neuroscience*, 33(2), 130-143.
- [4] Bernier, R., Aaronson, B., and McPartland, J. (2013). The role of imitation in the observed heterogeneity in EEG mu rhythm in autism and typical development. *Brain and cognition*, 82(1), 69-75.
- [5] Bernier, R., Dawson, G., Webb, S., and Murias, M. (2007). EEG mu rhythm and imitation impairments in individuals with autism spectrum disorder. *Brain and cognition*, 64(3), 228-237.
- [6] Bigdely-Shamlo, N., Mullen, T., Kothe, C., Su, K. M., and Robbins, K. A. (2015). The PREP pipeline: standardized preprocessing for large-scale EEG analysis. *Frontiers in neuroinformatics*, 9, 16.
- [7] Binnie, C. D., and Prior, P. F. (1994). Electroencephalography. Retrieved from <https://www.ncbi.nlm.nih.gov/pmc/articles/PMC1073178/pdf/jnmpsync00041-0006.pdf>

- [8] Blake, R., Turner, L. M., Smoski, M. J., Pozdol, S. L., and Stone, W. L. (2003). Visual recognition of biological motion is impaired in children with autism. *Psychological science*, 14(2), 151-157.
- [9] Carter, A. S., Black, D. O., Tewani, S., Connolly, C. E., Kadlec, M. B., and Tager-Flusberg, H. (2007). Sex differences in toddlers with autism spectrum disorders. *Journal of autism and developmental disorders*, 37(1), 86-97.
- [10] Cheng, Y., Lee, P. L., Yang, C. Y., Lin, C. P., Hung, D., and Decety, J. (2008). Gender differences in the mu rhythm of the human mirror-neuron system. *PLoS One*, 3(5), e2113.
- [11] Christensen, D. L., et al. (2016, April 1). Prevalence and Characteristics of Autism Spectrum Disorder Among Children Aged 8 Years – Autism and Developmental Disabilities Monitoring Network, 11 Sites, United States, 2012. Retrieved from <https://www.cdc.gov/mmwr/volumes/65/ss/ss6503a1.htm>
- [12] Cohen. (1959, March 4). Richard Caton (1842-1926): Pioneer Electrophysiologist. Retrieved from <https://www.ncbi.nlm.nih.gov/pmc/articles/PMC1870055/pdf/procrsmed00267-0091.pdf>
- [13] Delorme, A., and Makeig, S. (2004). EEGLAB: an open source toolbox for analysis of single-trial EEG dynamics including independent component analysis. *Journal of neuroscience methods*, 134(1), 9-21.
- [14] Di Pellegrino, G., Fadiga, L., Fogassi, L., Gallese, V., and Rizzolatti, G. (1992). Understanding motor events: a neurophysiological study. *Experimental brain research*, 91(1), 176-180.
- [15] Electroencephalogram (EEG). (n.d.). Retrieved from <http://www.hopkinsmedicine.org/>
- [16] Fombonne, E. (2005). The changing epidemiology of autism. *Journal of Applied Research in Intellectual Disabilities*, 18(4), 281-294.

- [17] Holmes, E. E. An EM algorithm for maximum likelihood estimation given corrupted observations.
- [18] Holtmann, M., Bölte, S., and Poustka, F. (2007). Autism spectrum disorders: Sex differences in autistic behaviour domains and coexisting psychopathology. *Developmental Medicine and Child Neurology*, 49(5), 361-366.
- [19] In, M. H., Lee, S. Y., Park, T. S., Kim, T. S., Cho, M. H., and Ahn, Y. B. (2006). Ballistocardiogram artifact removal from EEG signals using adaptive filtering of EOG signals. *Physiological measurement*, 27(11), 1227.
- [20] Jones, V., and Prior, M. (1985). Motor imitation abilities and neurological signs in autistic children. *Journal of autism and developmental disorders*, 15(1), 37-46.
- [21] Klin, A., Lin, D. J., Gorrindo, P., Ramsay, G., and Jones, W. (2009). Two-year-olds with autism orient to non-social contingencies rather than biological motion. *Nature*, 459(7244), 257-261.
- [22] Kopp, S., and Gillberg, C. (1992). Girls with social deficits and learning problems: Autism, atypical Asperger syndrome or a variant of these conditions. *European Child and Adolescent Psychiatry*, 1(2), 89-99.
- [23] Levin A.R., Mendez Leal A., O’Leary H.M. (2016). Boston EEG Automated Processing Pipeline [Computer software]. Boston, MA: Boston Children’s Hospital.
- [24] Martineau, J., Cochin, S., Magne, R., and Barthelemy, C. (2008). Impaired cortical activation in autistic children: is the mirror neuron system involved?. *International journal of psychophysiology*, 68(1), 35-40.
- [25] McLennan, J. D., Lord, C., and Schopler, E. (1993). Sex differences in higher functioning people with autism. *Journal of autism and developmental disorders*, 23(2), 217-227.

- [26] Molenberghs, P., Cunnington, R., and Mattingley, J. B. (2009). Is the mirror neuron system involved in imitation? A short review and meta-analysis. *Neuroscience and Biobehavioral Reviews*, 33(7), 975-980.
- [27] Morbidi, F., Garulli, A., Prattichizzo, D., Rizzo, C., Manganotti, P., and Rossi, S. (2007). Off-line removal of TMS-induced artifacts on human electroencephalography by Kalman filter. *Journal of neuroscience methods*, 162(1), 293-302.
- [28] Nicholas, J. S., Charles, J. M., Carpenter, L. A., King, L. B., Jenner, W., and Spratt, E. G. (2008). Prevalence and characteristics of children with autism-spectrum disorders. *Annals of Epidemiology*, 18(2), 130-136.
- [29] Nitschke, J. B., Miller, G. A., and Cook, E. W., III. (1998). Retrieved from <http://cb3.unl.edu/dbrainlab/wp-content/uploads/sites/2/2013/12/2a.-Nitschke-1998-Digital-filtering.pdf>
- [30] Oberman, L. M., Hubbard, E. M., McCleery, J. P., Altschuler, E. L., Ramachandran, V. S., and Pineda, J. A. (2005). EEG evidence for mirror neuron dysfunction in autism spectrum disorders. *Cognitive brain research*, 24(2), 190-198.
- [31] Oberman, L. M., McCleery, J. P., Hubbard, E. M., Bernier, R., Wiersema, J. R., Raymaekers, R., and Pineda, J. A. (2013). Developmental changes in mu suppression to observed and executed actions in autism spectrum disorders. *Social cognitive and affective neuroscience*, 8(3), 300-304.
- [32] Oberman, L. M., Ramachandran, V. S., and Pineda, J. A. (2008). Modulation of mu suppression in children with autism spectrum disorders in response to familiar or unfamiliar stimuli: the mirror neuron hypothesis. *Neuropsychologia*, 46(5), 1558-1565.
- [33] Pineda, J. A., Allison, B. Z., and Vankov, A. (2000). The effects of self-movement, observation, and imagination on/spl mu/rhythms and readiness potentials (RP's): toward a brain-computer interface (BCI). *IEEE Transactions on Rehabilitation Engineering*, 8(2), 219-222.

- [34] Raymaekers, R., Wiersema, J. R., and Roeyers, H. (2009). EEG study of the mirror neuron system in children with high functioning autism. *Brain research*, 1304, 113-121.
- [35] Rizzolatti, G., and Craighero, L. (2004). The mirror-neuron system. *Annu. Rev. Neurosci.*, 27, 169-192.
- [36] Saygin, A. P., Wilson, S. M., Hagler, D. J., Bates, E., and Sereno, M. I. (2004). Point-light biological motion perception activates human premotor cortex. *Journal of Neuroscience*, 24(27), 6181-6188.
- [37] Shumway, R. H., and Stoffer, D. S. (1982). An approach to time series smoothing and forecasting using the EM algorithm. *Journal of time series analysis*, 3(4), 253-264.
- [38] Tsai, L. Y., and Beisler, J. M. (1983). The development of sex differences in infantile autism. *The British Journal of Psychiatry*, 142(4), 373-378.
- [39] Tudor, M., Tudor, L., and Tudor, K. I. (2005). Hans Berger (1873-1941)—the history of electroencephalography. Retrieved from <http://europepmc.org/abstract/med/16334737>
- [40] Ulloa, E. R., and Pineda, J. A. (2007). Recognition of point-light biological motion: mu rhythms and mirror neuron activity. *Behavioural brain research*, 183(2), 188-194.
- [41] Welch, G., and Bishop, G. (2006). An introduction to the kalman filter. Department of Computer Science, University of North Carolina. *ed: Chapel Hill, NC, unpublished manuscript.*
- [42] Williams, J. H., Whiten, A., and Singh, T. (2004). A systematic review of action imitation in autistic spectrum disorder. *Journal of autism and developmental disorders*, 34(3), 285-299.
- [43] Yang, C. Y., Decety, J., Lee, S., Chen, C., and Cheng, Y. (2009). Gender differences in the mu rhythm during empathy for pain: an electroencephalographic study. *Brain research*, 1251, 176-184.